TSUNAMI INUNDATION DATABASE FOR JARAMIJÓ, ECUADOR

Leonardo Alvarado García* Supervisor: Shunichi Koshimura**
MEE16719

ABSTRACT

The Oceanographic Institute of the Ecuador Navy (INOCAR) is currently working on the development of a tsunami database to determine maximum tsunami height as well as time of arrival in different cities along the coastline. The main objective is to rapidly assess the possible consequences of the occurrence of a local tsunami. This study proposes the construction of a tsunami inundation database in Jaramijó city as an example to be replicated in other cities. The short-term objective is to link inundation maps to INOCAR's tsunami database for disseminating local tsunami warning bulletins. The TUNAMI-N2 code is used for simulation with bathymetry and topography data from GEBCO and INOCAR. A total of 564 scenarios were modeled considering four magnitudes (Mw = 9.0, 8.5, 8.0 and 7.5) at fault-top depths of 5, 10, 15 and 20 km. The worst-case inundation scenario is found when we model a Mw 9.0 earthquake at a depth of 20 km. This case could be taken as an example to work on a tsunami contingency plan in Jaramijó, considering that the worst tsunami scenario of the 1906 earthquake (Mw 8.8) occurred in the northern sea border of our territory.

Keywords: Tsunami Inundation Database, Tsunami Simulation, Inundation Map.

1. INTRODUCTION

Ecuador is located in south America on the east side of the Pacific Ocean, between 1.66º north and 5.01º south, close to the convergence zone where fast subduction of the oceanic Nazca plate beneath the South American (SoAm) continental plate causes large megathrust earthquakes (Nishenko, 1991). In the last century, five large megathrust earthquakes occurred in the Ecuador-Colombia subduction zone (Chlieh et al., 2014). One of these events was the 1906 Colombia-Ecuador earthquake which registered a moment magnitude of 8.8 and caused a tsunami that mostly affected the coasts of southern Colombia and northern Ecuador.

Due to a lack of historical information on earthquakes and considering that the implementation of a seismic network in Ecuador was only established about forty years ago, it is a challenge to conduct research with local data for the purposes of projecting possible long-term future earthquake scenarios as has been done in Japan. Due to the proximity of the trench to the coastline of Ecuador, the occurrence of any nearby seismic event might cause a tsunami that could affect coastal cities. The number of inhabitants has increased considerably in the last century. However, there has fortunately been no tsunami as destructive as that from the 1906 earthquake.

In this study, the 11 most populated cities located on the coastline were selected at first. Using 30 arc-sec resolution bathymetry from GEBCO and with the help of the tsunami linear code TUNAMI-N1, hypothetical Mw 9.0 scenarios were modeled in front of every city. The determination of the fault parameters to be used for theses simulations were determined by using the scaling law from Papazachos et al. (2004) for dip-slip faults in subduction regions.

* Oceanographic Institute of Ecuador Navy (INOCAR), Guayaquil, Ecuador.
** International Research Institute of Disaster Science (IRIDES), Tohoku University, Japan.

Once every scenario was modeled, all water elevation values obtained from the synthetic observation points were analyzed to determine the city with the highest tsunami risk. Jaramijó was finally chosen as the target area of the tsunami inundation database.

2. DATA

For tsunami modeling, five domains including the target area (Domain 5) are prepared with bathymetry and topography data in different resolution. The spatial resolution plays a very important role in the simulation since the detail in the target area will allow a more realistic representation of any scenario. The geographic coordinates of these domains as well as the properties for computational purpose are shown in Table 1.

Table 1. Geographic coordinates and properties for computational domains.

Grid	Longitude						Latitude						Spatial Resolution		Dimension	
	West			East			South			North			m	arc-sec	IF	JF
	deg	min	sec	deg	min	sec	deg	min	sec	deg	min	sec				
1	-82	28	49.8	-78	46	58.8	-3	37	35.4	2	54	21.6	810	27	493	871
2	-81	5	42.0	-80	33	36	-1	0	39.6	-0	28	33.6	270	9	214	214
3	-80	46	44.76	-80	35	44.8	-0	58	49.17	-0	50	31.17	90	3	220	166
4	-80	44	1.61	-80	36	3.6	-0	58	43.61	-0	52	33.61	30	1	478	370
5	-80	41	20.43	-80	36	18.1	-0	58	26.33	-0	54	18	10	0.33	907	745

For domains 1 and 2, bathymetry and topography data from the General Bathymetric Chart of the Oceans (GEBCO) was used. Since very detailed data was needed to produce a more realistic output; for domains 3 to 5, the data was obtained from the Oceanographic Institute of Ecuador Navy (INOCAR). The output raster datasets of these domains are shown in Figure 1.

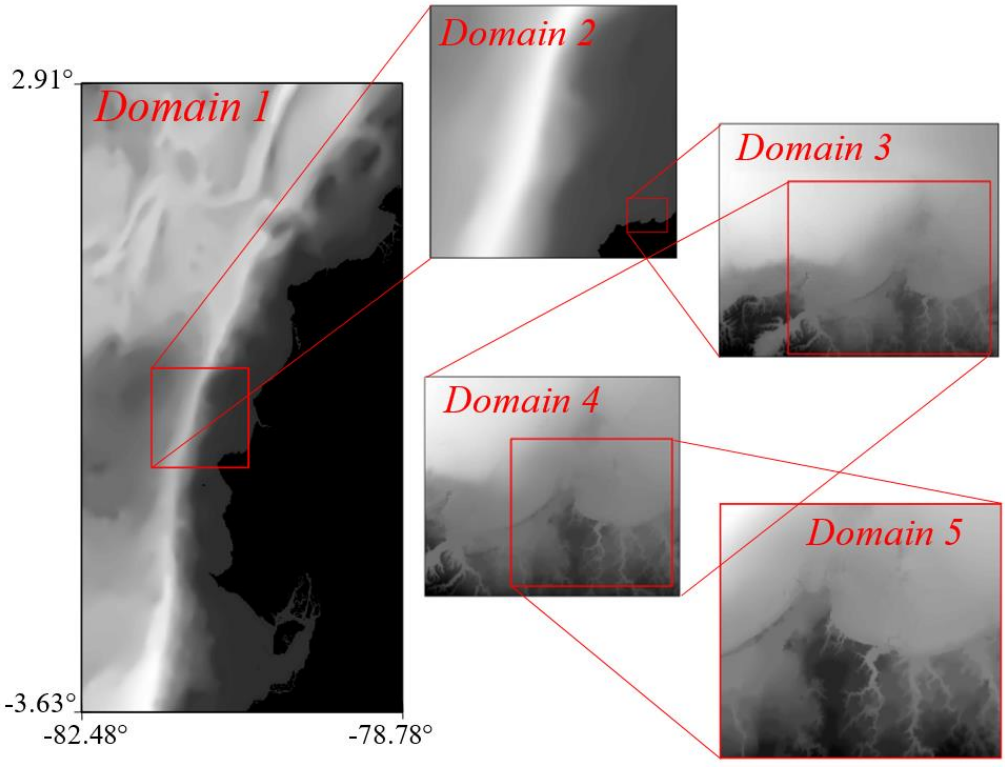

Figure 1. Raster datasets of computational domains used for tsunami inundation modeling.

3. METHODOLOGY

As part of a cooperation project between Ecuador and Japan, INOCAR and JICA started working on a database with local precomputed scenarios that allow the assessment of coastal tsunami risk. This tsunami evaluation system was named “Hatysa” and started in 2015. This system is being developed in order to make possible the determination of maximum wave height and arrival time in different places. The domain of the synthetic epicenters for Hatysa system was created by combining the results obtained from Kernel Density Estimation of the area of interest and the depth of the slab. Furthermore, with the help of an automatic mesh generator, the location of the epicenters in the delimited domain was established. Once all the necessary values were established for the purpose of modeling, INOCAR’s database comprised 185 synthetic epicenters. The magnitude range of INOCAR database is from 6.0 to 9.0 with an increment of 0.1, giving a total of 22,133 scenarios. As they were most relevant, we only execute the scenarios with magnitudes of 9.0, 8.5, 8.0 and 7.5. And also we only used the source depths of 5, 10, 15 and 20 km because the slab is equal or lower than 20 km deep. Overall, 564 scenarios were generated.

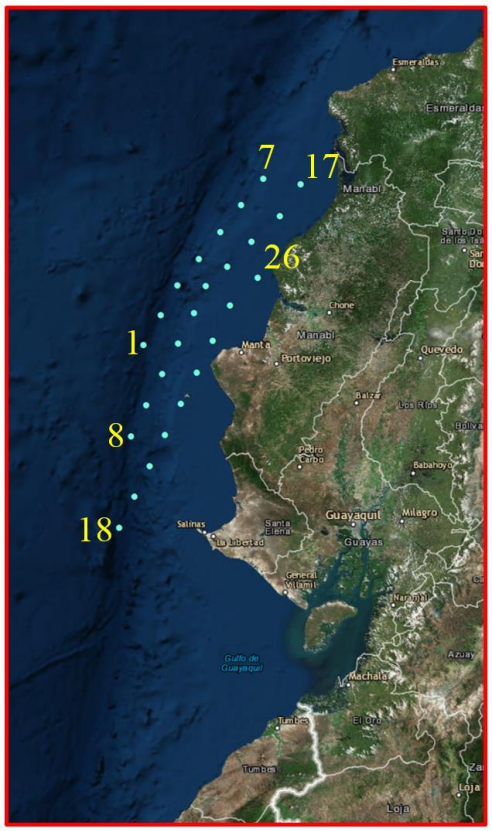

Figure 2. Source locations of simulated scenarios for Mw 9.0 earthquake. Topography image is from Google Maps.

Epicenters from Hatysa were considered as a constant, but the length, width and slip of the fault plane differed for each magnitude. A total of 26 scenarios were modeled for the first trial (Mw 9.0 at depth of 5 km), as seen in Figure 2.

Using the focal mechanism parameters, the vertical elastic deformation model (Okada, 1985) was taken into consideration of the initial condition for tsunami simulation. This model requires the latitude and longitude of the fault plane origin, its length and width, strike, dip, rake, slip and depth of the source.

The Tohoku University’s Numerical Analysis Model for Investigation of Near-field tsunamis (TUNAMI-N2) was used for this study. This code was originally developed in the Disaster Control Research Center of Tohoku University and could be used to compute the water surface elevation and velocities due to tsunami across the entire computational domain, including shallow water and land regions.

4. RESULTS AND DISCUSSION

The tsunami inundation database helps to determine the worst-case scenario in the target area. For the case of Jaramijó, the worst-case scenarios were determined by comparing the values for each magnitude and depth. The same procedure was applied to the rest of magnitudes and depths. The seafloor deformation and the worst-case inundation scenario for a Mw 9.0 earthquake is shown in Figure 3. The seafloor deformation and the tsunami inundation caused by the Mw 9.0 earthquake shows that the most inundated areas are located near the coastline where there is a considerable uplift. The impact on the population is visible where the inundation depth reaches up to 3 meters.

Once the inundation area was determined, with the availability of the topography features, it became easier to determine the run-up height at different points. For this, 12 random points were selected

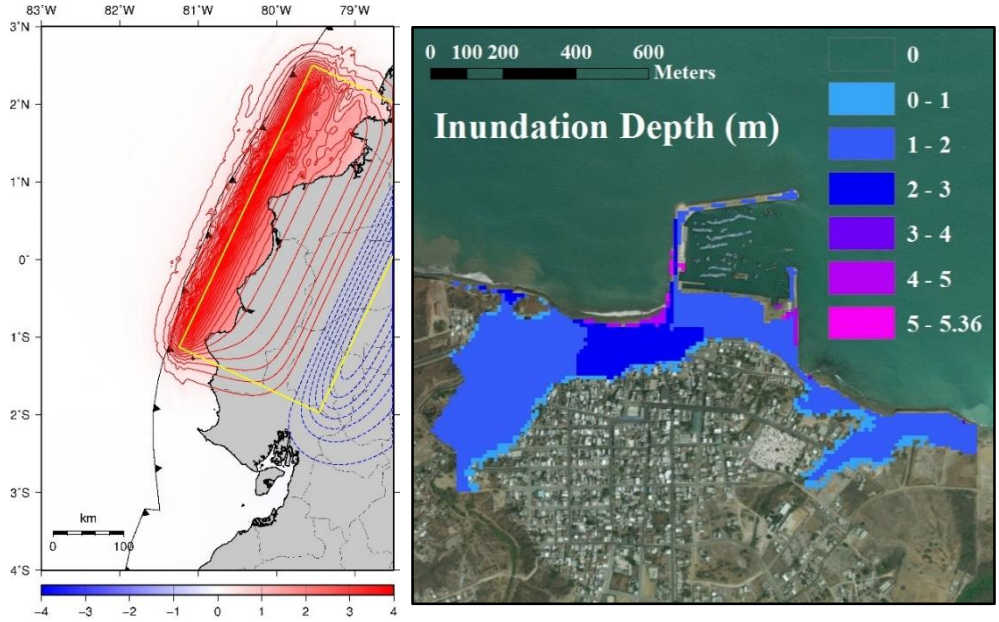

Figure 3. Seafloor deformation (contour interval of 0.1m) and inundation map of Jaramijó for Mw 9.0 earthquake at depth of 20 km (Scenario 22). Topography image is from Google Maps.

along the boundary of the inundated zone in order to clarify the impact of the tsunami, as seen in Figure 4. The maximum run-up height is located at point 9 with an elevation of 8.40 meters. This was due to the presence of a cliff, approximately 10 meters high, south of the fishing port. Fortunately, this area is relatively unpopulated compared to the region bounded by points 1 to 6 where the farthest inundation was registered at point 4 with the run-up height of 1 meter. The most affected area was located north of points 7 and 8 where the maximum inundation depth was 3 meters and the maximum run-up height was

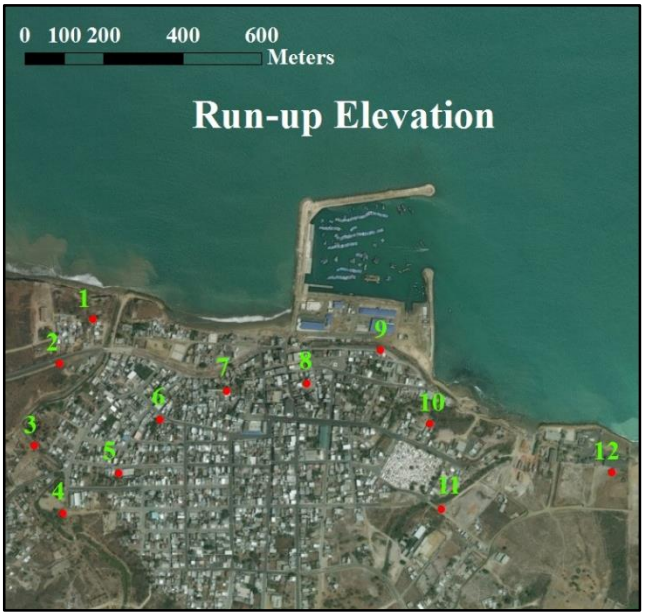

Point	Elevation (m)	Point	Elevation (m)
1	3.70	**7**	3.61
2	2.32	**8**	4.63
3	1.00	**9**	8.40
4	1.00	**10**	6.58
5	4.18	**11**	3.90
6	3.56	**12**	1.00

Figure 4. Run-up elevations in Jaramijó from a scenario of Mw 9.0 earthquake at depth of 20 km (Scenario 22). Topography image is from Google Maps.

4.63 meters. Finally, from points 10 to 12 where the maximum run-up height was 6.58 meters, there was no considerable risk due to the very low population density. As the representation of a worst-case scenario, the determination of these points may be useful for deciding locations for the construction of shelters or evacuation sites.

When we compare the scenario for a Mw 9.0 earthquake with the worst-case scenario for a Mw 8.5 earthquake, the latter shows no considerable seafloor uplift as seen in Figure 5. Also, the maximum inundation depth drastically decreases, but inundate on heights at populated areas only up to 2.28 meters.

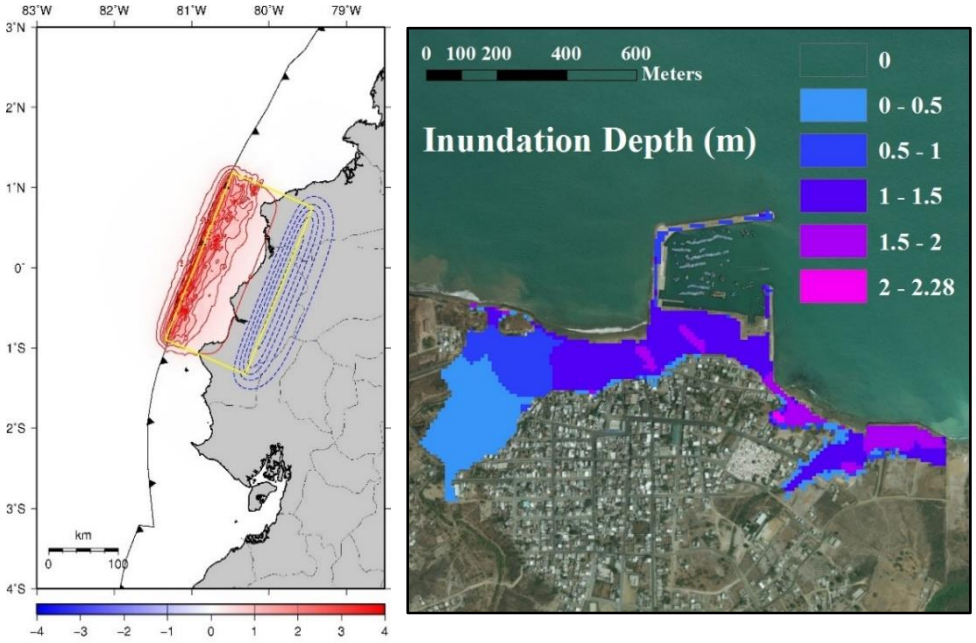

Figure 5. Same as Figure 3 but for a Mw 8.5 earthquake at depth of 10 km.

The worst-case scenario for a Mw 8.0 earthquake is shown in Figure 6. The dimension of the fault plane and the slip decreased to just over a third of the Mw 9.0 scenario. It was observed that there is minimum subsidence in Jaramijó and that the maximum inundation depth was 2 meters.

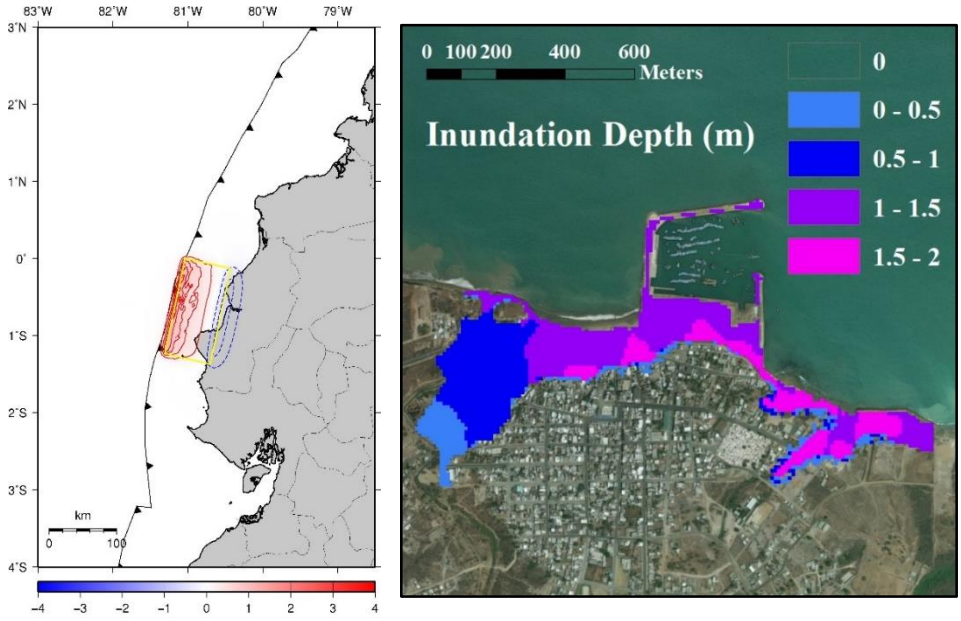

Figure 6. Same as Figure 3 but for a Mw 8.0 earthquake at depth of 5 km.

For the scenarios (Mw 9.0, 8,5 and 8.0) described above, the farthest inundated areas were located approximately 1 kilometer away from the coastline, suggesting therefore that the establishment of safety shelters should be beyond this point. In this study, only 564 scenarios out of 22,133 were modeled. There is the possibility that other scenarios not generated in this study might cause worse

consequences than those described here. The procedure in this study can be replicated for other coastal cities to determine tsunami risk scenarios. Despite the fact that a real-time inundation forecast system is not available, the results might help to strengthen any tsunami disaster mitigation plan, infrastructure and increase awareness.

5. CONCLUSIONS

This study includes two main approaches, linear and non-linear tsunami modeling. The linear approach was used to determine the risk in tsunami-prone urban areas. Once Jaramijó was selected as the target area for this study, bathymetry and topography data from INOCAR and GEBCO were used for domains 3 to 5 and for domains 1 and 2, respectively.

Fault parameters were obtained from the INOCAR tsunami database which has 22,133 scenarios. Out of these scenarios, 564 were considered for this study. Seafloor deformation for the five domains were calculated following Okada's (1985) model.

The inundation depth obtained from the TUNAMI-N2 code execution were sorted according to earthquake magnitudes (9.0, 8.5, 8.0 and 7.5) and fault depth (5, 10, 15 and 20 km). The final outputs were compared, and finally the worst-case scenarios were obtained for each magnitude and depth.

This study is a small step towards developing a proper tsunami inundation database and contribution to raising awareness of tsunami risks. The implementation of a proper tsunami database and an inundation database is the next objective for the improvement of the tsunami warning system in Ecuador. In the future, these efforts will contribute to strengthen tsunami mitigation capabilities and minimize casualties along the coast.

ACKNOWLEDGEMENTS

I would like to express my sincere gratitude to Dr. Shunichi Koshimura for giving me the opportunity to work alongside his staff at Tohoku University and for making available the tools for me to complete my thesis. Thanks are also due to Dr. Bruno Adriano for supervising me and giving me very useful advice and suggestions during my individual study, and Dr. Eric Mas for his support during this process.

I would also like to acknowledge Dr. Yushiro Fujii and the staff members of IISEE/BRI for their support during my stay in Japan, and the Japan International Cooperation Agency (JICA) for facilitating my participation in this course and financing this program.

REFERENCES

Chlieh, M., Mothes, P. A., Nocquet, J. M., Jarrin, P., Charvis, P., Cisneros, D. & Vallée, M. (2014). Distribution of discrete seismic asperities and aseismic slip along the Ecuadorian megathrust. *Earth and Planetary Science Letters*, *400*, 292-301.

Nishenko, S. P. (1991). Circum-Pacific seismic potential: 1989–1999. In *Aspects of Pacific Seismicity* (pp. 169-259).

Okada, Y. (1985). Surface deformation due to shear and tensile faults in a half-space. *Bulletin of the seismological society of America* 75.4: 1135-1154.

Papazachos, B., Scordilis, E., Panagiotopoulus, D., Papazachos, C., & Karakaisis, G. (2004). Global relations between seismic fault parameters and moment magnitude of earthquakes. In *Bulletin of the Geological Society of Greece, 36(3),* 1482-1489.